Response of an Indented Square Tube under Impact Loading

Z. H. Tan,[a,1] L. S. Liu,[a] Y. S. Sun,[b] and C. Cho[c]

[a] Department of Structure Engineering and Mechanics, School of Science, Wuhan University of Technology, Wuhan, China

[b] College of Mechanical and Vehicle, Hunan University, Changsha, China

[c] Department of Mechanical Engineering, College of Engineering, Inha University, Incheon, Republic of Korea

[1] zhtan@whut.edu.cn

The dynamic buckling of the square tube with a V-shape indent under impact loading was investigated by experimental and numerical methods. The collapse modes of square tubes with different locations of indentation points were obtained experimentally. Numerical calculations of each experimental load case were conducted to analyze the effect of the indentation point location on the crush force and energy absorption of the tube. Numerical results agree well with the experimental ones. The results show that the indentation point location exerts a significant influence on the crush force and energy absorption. Compared to an indentation-free tube, the peak force of the indented tube is evidently reduced. The collapse process of the tube includes two buckling steps. The first one begins from the indentation either forward or backward with respect to the end until the folds are densified, then the second buckling starts backward or forward, which results in a second peak force in the collapse process.

Keywords: square tube, indentation, collapse mode, crush force, energy absorption.

Introduction. Thin-walled structures have been widely used as energy absorbers and lightweight components in civil engineering and military applications [1]. For example, various thin-walled structures are designed to reduce the crash force and absorb the impact energy during automobile crashes or spacecraft landings.

Numerous studies have been dedicated to the axial crush behavior and collapse mechanisms of thin-walled tubes under quasi-static and impact loadings using various theoretical, experimental, and numerical methods [2–9], which imly the impact energy dissipation via reliable and stable collapse deformation modes. Some researchers report that there is an extreme crush peak force during the initial buckling of the tube, which can cause the excessive deceleration and severe injury to a protected person or object [10, 11].

In order to resolve this issue, the trigger configuration was designed to reduce the initial crush peak force and achieve the stable collapse modes, such as the extensional or inextensional ones [12]. Various types of triggers, such as corrugation [13, 14], groove [15], dent [16], discontinuity [17], and buckling initiator [18] have been studied form the viewpoint of the cylindrical or square tube buckling response. However, the dynamic buckling behavior of an indented tube under impact loading remains an open problem.

In this study, the dynamic response of Q235 steel square tubes with a V-shape indentation is investigated. The square tube is impacted by a cylindrical steel projectile at the velocity in the range of 9.00 to 13.18 m/s. The dynamic deformation evolution is recorded with a high-speed camera, and various collapse modes are revealed for the different load cases. The numerical simulation of the impact test is also performed, in order to analyze the crush force and energy absorption. A comparative analysis of the experimental and numerical results is used to assess the collapse mechanism of an indented square tube under impact loading conditions. In addition, the indentation location effects on the collapse mode, crush force and energy absorption are discussed.

1. Experimental.

1.1. Specimen. The Q235 steel square tube dimensions are as follows: the square cross section is of 20×20 mm, while the wall thickness (t) and length (L_0) are 0.5 and 100 mm, respectively.

The V-shaped indentation is pressed into the two opposite faces of the specimen. Four different indentation locations are designed in the specimens with the distances from the impacted end to the indentation L of 12, 24, 36, and 64 mm, respectively. The V-shaped indentation dimensions are: 2 mm in width (w) and 1 mm in depth (h), as shown in Fig. 1.
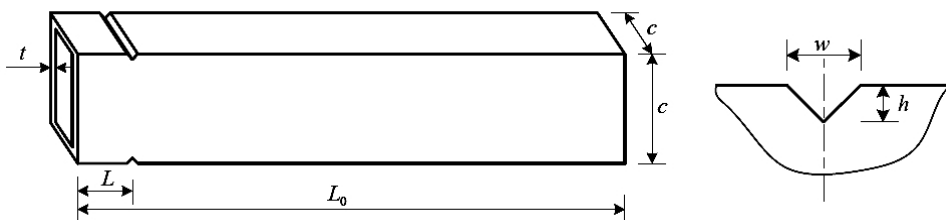

Fig. 1. The square tube with V-shape indentation.

1.2. Impact Test. A cylindrical steel projectile is launched via a gas gun and impacted at the square tube, the impact velocity being measured by a laser velocimeter. The steel square tube end is glued to the rigid wall, which is treated as a fixed constraint. The mass of the steel projectile is 4.95 kg, while the motion velocity of the projectile ranges from 9.0 to 11.85 m/s, as is shown in Table 1. An FASTCAM-SA5 high-speed camera with the frame rate set to 7,000 fps is used to record the deformation process of the square tubes in the impact test. The experimental setup is shown in Fig. 2.

T a b l e 1

Specimens and Experimental Load Cases

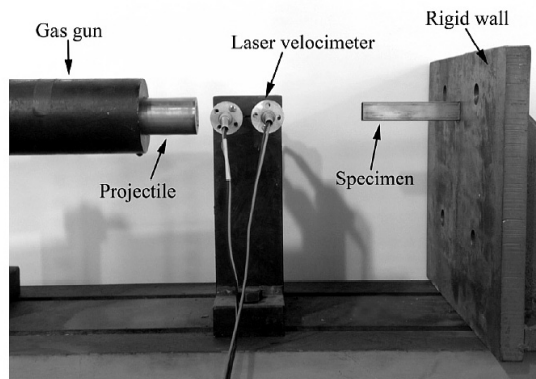| Case No.	Indentation location (mm)	Impact velocity (m/s)
1	0	10.17
2	12	9.85
3	24	10.05
4	36	9.83
5	64	10.20

Fig. 2. The impact device for the impact experiments.

2. Numerical Model. The numerical simulation of the experimental load case is performed using the ANSYS LS-DYNA 970 commercial software. The square tube is modeled using the Belytschko–Tsay 4-node shell elements with five integration points through the thickness and one integration point within the element, while the projectile FEM-mesh is constructed using 8-node solid elements. The shell element size for the simulated square tube is about 1 mm. The clamped boundary condition is applied directly at the square tube bottom to simulate the square tube fixation to the rigid wall. The projectile velocities in calculations correspond to the experimental ones for various load cases under study.

An automatic single-surface contact algorithm is applied in the simulation to account for the contact between the tube walls throughout the deformation process, and an automatically-adjusted node between the tube and the projectile is used in the surface contact algorithm. The dynamic and static friction coefficients of 0.2 are used for the self-contact of the square tube walls and for the tube-projectile contact.

A similar tube of the same material (Q235 steel) was also studied in [19], where the material model #103 in the LS-DYNA code was applied. The respective parameters of this model, which are used in the present study, are listed in Table 2.

T a b l e 2

Parameters of #103 Material Model [19]

E, GPa	μ	σ_Y, MPa	σ_u, MPa	C_1, MPa	C_2, MPa	Q_1, MPa	Q_2, MPa
210	0.28	218	323.3	46.1	4.24	43.9	233.3

3. Results and Discussion.

3.1. Buckling Process Results and Their Validation. The five load cases with different indenation locations and impact velocities (Table 1) were experimentally investigated, whereas each load case was tested twice to ensure the reliability of the results. The respective numerical simulatons were also performed, and their results were compared with respective experimental ones.

Figure 3 shows the deformation process of the tube without an indentation (Case 1). The dynamic progressive buckling of the tube starts from the proximal end, while the collapse mode is inextensional. The numerical results are in agreement with the experimental data implying the final length of the deformed tube of 64 mm.

Figure 4 illustrates the results of Case 2. Here the numerical results also agree well with the experimental datas. It is obvious that the onset of the collapse is at the indentation position, which is followed by the progressive buckling from the indentation location towards the proximal end. It is clear that the indentation efficiently induced the progressive collapse, while the final length of the deformed tube is 44.8 mm.

Figures 5 and 6 show the collapse progress of the tube in Cases 3 and 4, respectively. The deformation processes in these cases are similar: the tube is subdivided into the front and rear parts by the indentation, while the total buckling process includes two steps. The first step starts from the indentation location and proceeds backward to the proximal end, as is shown in Figs. 5b–c and 6b–c. The first-step progressive buckling is terminated, when the folds are densified, as shown in Figs. 5d and 6d, and the second step starts. The second-step progressive buckling proceeds from the indentation location toward the distal end. The experimental final length of the deformed tube is 49.2 mm.

Figure 7 presents the collapse process of Case 5, which is similar to those of Case 3 and 4, and includes the same two steps. The first-step progressive buckling proceeds from the indentation location to the distal end until the folds are densified in the rear part of the tube. Then the second-step progressive buckling starts from the indentation position and proceeds to the proximal end. The experimental final length of the deformed tube is 69.3 mm.
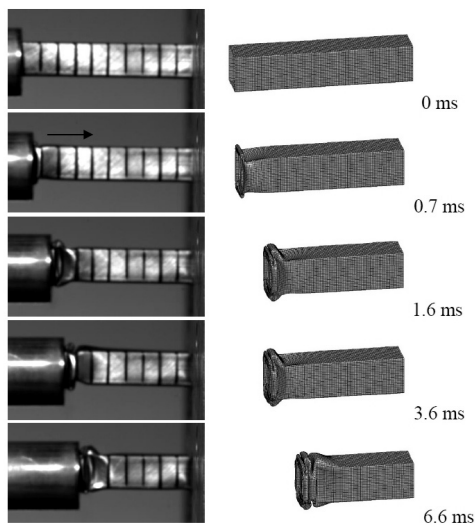
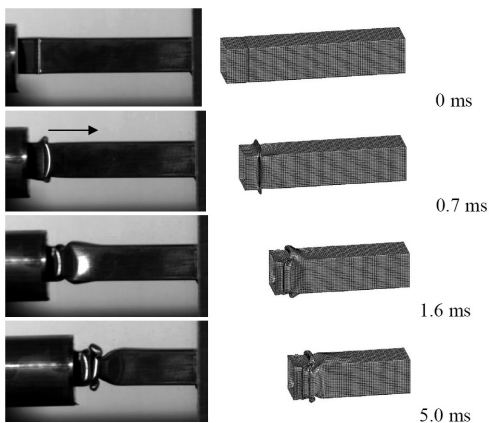Fig. 3. The deformation process of Case 1.
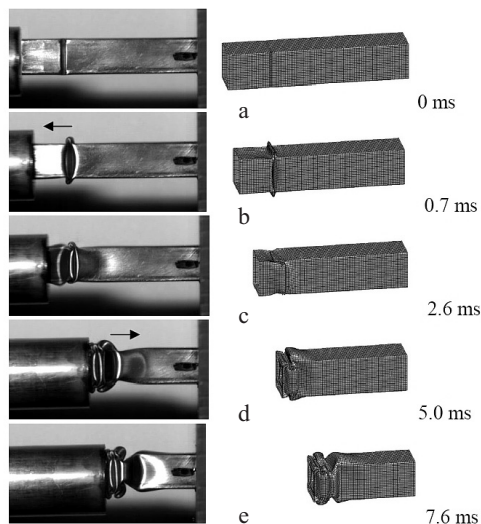

Fig. 4. The deformation process of Case 2.
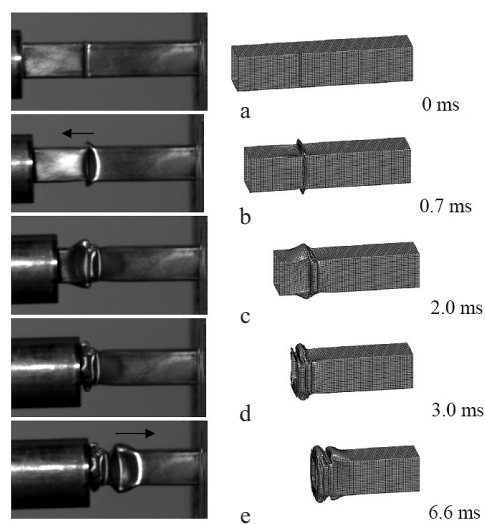

Fig. 5. The deformation process of Case 3.

Fig. 6. The deformation process of Case 4.

3.2. Crush Load. The numerical results exhibit a close correlation with the experimental ones, which proves the validity of the applied numerical model. Therefore, this numerical model was used to analyze the effect of indentation location on the crush load and energy absorption values. Since the above effect should be assesed for the same impact velocities, the models for Cases 1–5, which were used in the subsequent Sections, were modified to simulate the projectile with the same impact velocity of 10 m/s compressing the tube until the displacement of the projectile is 800 mm. Figure 8 presents the crush load values for the tube in the different cases.

The square tube buckling behavior for different load cases is shown in Table 3. As compared to the peak force 19.1 kN of the tube without an indentation, the one of the tube with an indentation exhibits a reduction by 14.1 to 25.7%. When the distance from the proximal end to the indentation location is increased, the peak force of the tube with an indentation also increases from 14.2 to 16.4 kN. Moreover, there is a second peak force in

T a b l e 3

Performance of Square Tube for Different Load Cases

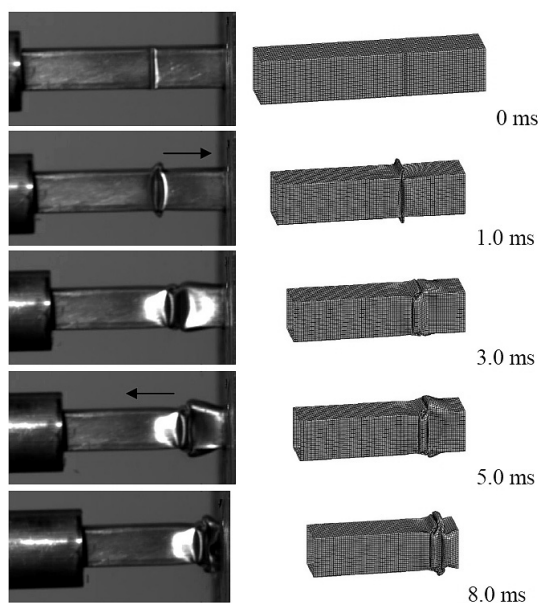| Case No.	Peak force (kN)	The second peak force (kN)	Mean crushing force (kN)	Energy absorption (J)
1	19.1	–	39.00	312
2	14.2	–	42.38	339
3	14.3	8.49	41.38	331
4	15.1	9.24	40.62	325
5	16.4	7.43	42.13	337

Fig. 7. The deformation process of Case 5.

Cases 3–5 (Fig. 8c–e), which is not observed in doesn't occur in Cases 1 and 2 (Fig. 8a, b). This can be explained as follows: when the first-step progressive buckling is terminated, the folds are densified at the proximal (Cases 3 and 4) or distal (Case 5) ends, as is shown in Fig. 8c–e. At this moment, the deformed tube can be considered as a new one with a densified end. The tube starts to buckle again from the densified end, which results in the second peak force appearance. This agrees well with the phenomenon observed in Figs. 5–7. However, the progressive buckling is fully developed in Cases 1 and 2, in contrast to Cases 3–5. Thus, there the second peak force is missing in Cases 1 and 2.

   3.3. Energy Absorption. The energy absorption is defined as follows [19]:

$$E = \int_0^\delta F d\delta,$$

where F and δ are the crushing force and displacement, respectively. The mean crushing force is one of the major parameters controlling the efficiency of the energy-absorbing devices. The mean crushing force F_m is calculated as in [19]:
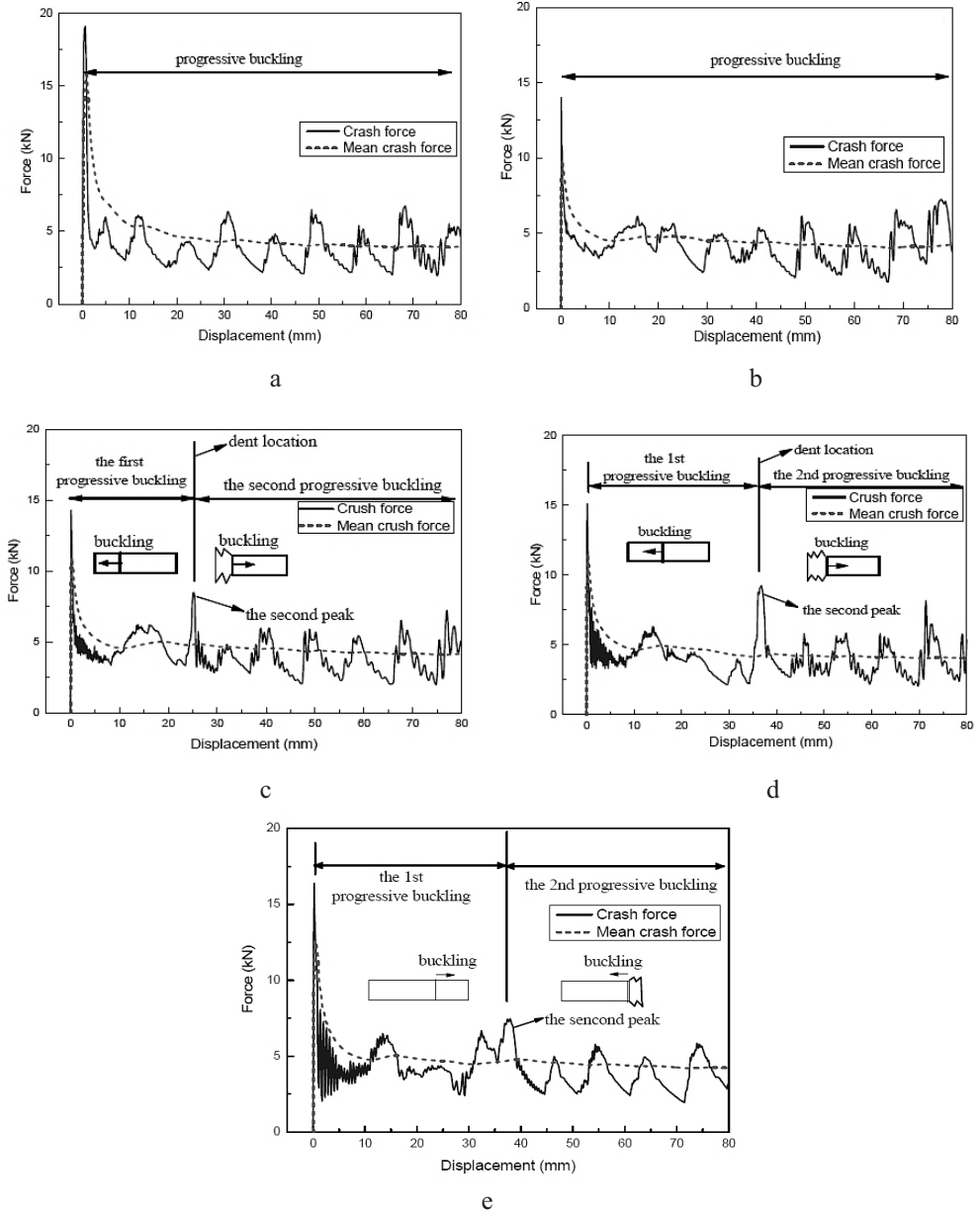
a

b

c

d

e

Fig. 8 Curves of crush force vs. displacement for different load cases at the velocity of 10 m/s: (a) Case 1; (b) Case 2; (c) Case 3; (d) Case 4; (e) Case 5.

$$F_m = \frac{1}{\delta} \int_0^{\delta} F d\delta.$$

Figure 9 shows that there is no obvious difference in the energy absorption values of the tube in various cases. The comparative analysis of the results listed in Table 3 and depicted Fig. 9 reveals that the energy absorption of the tube without indentation (Case 1) is the minimum. As compared to Case 1, the energy absorption in other cases is higher by 4.2 to 8.6%, which agrees well with the variation tendency of the mean force. This can be
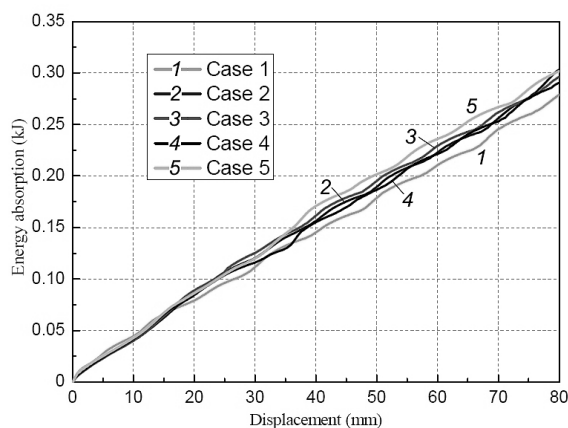
Fig. 9. Energy absorption–displacement curves for different load cases.

attributed to the following fact: although presence of the indentation decreases the initial peak force, it also changes the fold wavelength. Moreover, the densification of the first-step progressive buckling also contributes to the increase in energy absorption of a tube with an indentation.

Conclusions. The dynamic response of the tube with an indentation was studied by the experimental and numerical methods. The peak force and energy absorption values of an indented tube were compared to those of a tube with no indentation. The performed analysis of the deformation mechanism allow us to draw the following conclusions:

1. As compared to a tube with no indentation, the initial peak force of the indented tube can be reduced by 14.1 to 25.7%, whereas the respective energy absorption can be increased by 4.2 to 8.6%.

2. The indentation location has a strong effect on the peak force and energy absorption values.

3. The progressive buckling of the indented tube in Cases 3 and 4 consists of two buckling steps.

4. The densification of folds in the first buckling step results appearance of the second peak crush force, which is considered as the additional contribution to the increase in the energy absorption.

1. A. A. A. Alghamdi, "Collapsible impact energy absorbers: an overview," *Thin-Wall. Struct.*, **39**, No. 2, 189–213 (2001).

2. T. Wierzbicki and W. Abramowicz, "On the crushing mechanics of thin-walled structures," *J. Appl. Mech.*, **50**, No. 4, 727–734 (1983).

3. W. Abramowicz and N. Jones, "Dynamic axial crushing of square tubes," *Int. J. Impact Eng.*, **2**, No. 2, 179–208 (1984).

4. D. H. Chen and S. Ozaki, "Numerical study of axially crushed cylindrical tubes with corrugated surface," *Thin-Wall. Struct.*, **47**, No. 11, 1387–1396 (2009).

5. D. Al Galib and A. Limam, "Experimental and numerical investigation of static and dynamic axial crushing of circular aluminum tubes," *Thin-Wall. Struct.*, **42**, No. 8, 1103–1137 (2004).

6. H. Zhao and S. Abdennadher, "On the strength enhancement under impact loading of square tubes made from rate insensitive materials," *Int. J. Solids Struct.*, **41**, No. 24-25, 6677–6697 (2004).

7. W. Abramowicz and N. Jones, "Transition from initial global bending to progressive buckling of tubes loaded statically and dynamically," *Int. J. Impact Eng.*, **19**, No. 5-6, 415–437 (1997).

8. D. Karagiozova, "Dynamic buckling of elastic–plastic square tubes under axial impact – I: stress wave propagation phenomenon," *Int. J. Impact Eng.*, **30**, No. 2, 143–166 (2004).

9. D. Karagiozova and N. Jones, "Dynamic buckling of elastic–plastic square tubes under axial impact – II: structural response," *Int. J. Impact Eng.*, **30**, No. 2, 167–192 (2004).

10. M. Langseth and O. S. Hopperstad, "Static and dynamic axial crushing of square thin-walled aluminium extrusions," *Int. J. Impact Eng.*, **18**, No. 7-8, 949–968 (1996).

11. Ø. Jensen, M. Langseth, and O. S. Hopperstad, "Experimental investigations on the behaviour of short to long square aluminum tubes subjected to axial loading," *Int. J. Impact Eng.*, **30**, No. 8-9, 973–1003 (2004).

12. X. Zhang and H. Huh, "Crushing analysis of polygonal columns and angle elements," *Int. J. Impact Eng.*, **37**, No. 4, 441–451 (2010).

13. D. H. Chen and S. Ozaki, "Circumferential strain concentration in axial crushing of cylindrical and square tubes with corrugated surfaces," *Thin-Wall. Struct.*, **47**, No. 5, 547–554 (2009).

14. A. A. Singace and H. El-Sobky, "Behaviour of axially crushed corrugated tubes," *Int. J. Mech. Sci.*, **39**, No. 3, 249–268 (1997).

15. S. J. Hosseinipour and G. H. Daneshi, "Energy absorption and mean crushing load of thin-walled grooved tubes under axial compression," *Thin-Wall. Struct.*, **41**, No. 1, 31–46 (2003).

16. S. Lee, C. Hahn, M. Rhee, and J. Oh, "Effect of triggering on the energy absorption capacity of axially compressed aluminum tubes," *Mater. Design*, **20**, No. 1, 31–40 (1999).

17. Q. W. Cheng, W. Altenhof, and L. Li, "Experimental investigations on the crush behaviour of AA6061-T6 aluminum square tubes with different types of through-hole discontinuities," *Thin-Wall. Struct.*, **44**, No. 4, 441–454 (2006).

18. X. W. Zhang, H. Su, and T. X. Yu, "Energy absorption of an axially crushed square tube with a buckling initiator," *Int. J. Impact Eng.*, **36**, No. 3, 402–417 (2009).

19. X. Zhang and H. Zhang, "Experimental and numerical investigation on crush resistance of polygonal columns and angle elements," *Thin-Wall. Struct.*, **57**, No. 8, 25–36 (2012).